

# MODELING URBAN THERMAL ANISOTROPY

J. A. Voogt<sup>a,\*</sup>, E. S. Krayenhoff<sup>a</sup>

<sup>a</sup> Department of Geography, University of Western Ontario, London ON N6A 5C2 Canada -[javoogt@uwo.ca](mailto:javoogt@uwo.ca)

**KEY WORDS:** surface temperature, anisotropy, urban climate, sensor-view model

## ABSTRACT:

Thermal remote sensing of urban areas is affected by directional variations (anisotropy) of the upwelling thermal radiation. The anisotropy arises due to the three-dimensionally rough urban surface that creates microscale patterns of surface temperature variability associated with surface position, orientation and composition, coupled with a biased view of this rough surface by the remote sensor. The large magnitudes of observed urban thermal anisotropy suggest it can be a significant factor in the interpretation of urban surface characteristics such as the surface urban heat island and application of urban surface temperatures to modelling urban surface heat fluxes. Here we couple the SUM urban surface sensor view model (Soux et al. 2004) with the urban canopy energy balance model of Mills (1997) and a newly developed three-dimensional energy balance model to investigate the variability of thermal anisotropy with surface geometric parameters. Relatively large anisotropy is modelled for realistic urban H/W ratios, and realistic plan area ratios generate a 30% variability of the thermal anisotropy over urban surfaces. Coupled simulations with both energy balance models yielded similar results for anisotropy in the case study examined. The simulations substantially underestimated the anisotropy compared to observations from a helicopter-mounted thermal scanner despite showing good agreement between modelled and observed temperature differences between major urban surface facets. This suggests the simplified urban surface geometry used by the models is inadequate to replicate the observed anisotropy.

## 1. INTRODUCTION

Anisotropy (directional variation) of upwelling thermal radiation complicates remote sensing of urban surface temperatures. The anisotropy is created through the combination of a three-dimensionally rough urban surface, sensor viewing geometry and varying solar loading (daytime) or cooling (night time) that creates strong microscale contrasts of surface temperature that depend on facet orientation and type. Urban thermal anisotropy has been observed (e.g. Lagouarde et al. 2004, Voogt and Oke 1998) and shown to be large with respect to the anisotropy of other natural or agricultural surfaces.

Direct observations of urban thermal anisotropy are expensive, typically necessitating aircraft based sensors to provide suitable spatial resolution and control over viewing direction. These costs generally preclude high temporal resolution assessments of multiple land uses or different cities. To expand our knowledge, the construction of numerical models that can represent the urban thermal anisotropy is needed. One such model is the SUM surface-sensor-sun relations model Soux *et al.* (2004). This model calculates how a remote sensor views a simple urban surface by calculating the *radiative source area* or view factors of the urban surface components for a given remote sensor position. When combined with surface temperature information, it is able to estimate the anisotropy of radiative temperature as seen by a given sensor-sun-surface configuration.

Results from SUM to date have been constrained by the availability of observed surface temperatures for specific urban geometries. Comprehensive observations of urban surface temperature that are necessary to initialize SUM are not commonly available, further limiting the assessment of urban thermal anisotropy. One approach to overcoming this

limitation is to model the urban surface temperatures. To study thermal anisotropy this requires a three-dimensional representation of the urban surface, so that the facet surface temperatures required for SUM are available. Here, the urban canopy layer climate model (UCLM) of Mills (1997) is used to estimate surface temperatures for a range of simple urban geometries that are then modelled by SUM and a newly available 3-D temperatures of urban facets (TUF-3D) model is also tested. This modelling approach provides the basis for investigating how urban thermal anisotropy varies as urban surface geometry changes.

While the limited observations over cities to date do provide some insight into the variations of anisotropy over different urban surfaces, modelling is necessary in order to better determine whether general relationships can be derived between the anisotropy and surface structure. Further, models provide the capability to extending our knowledge of urban thermal anisotropy to other seasons and locations. The combined urban sensor-view-energy-balance model simulations provide for the investigation of effective thermal anisotropy and its dependence on a range of determinants in a fully simulated environment.

## 2. METHODS

### 2.1 Study Sites

Simulations are performed based on two land use types for which direct observations of thermal anisotropy are available: a light industrial area (LI) and a downtown area (DT) in Vancouver BC Canada. Simulations are performed for the study areas with using the actual (area-averaged) surface geometries that correspond with the observed data (base-case)

---

\* Corresponding Author: James Voogt. E-mail: [javoogt@uwo.ca](mailto:javoogt@uwo.ca)

and then modifying the surface geometry to represent a range of actual and/or potential urban surface structures.

In each case, the urban surface is represented using a simple array of rectangular geometric shapes to represent the “buildings”. For simplicity, the building footprints are square in these simulations. The surface geometric characteristics of the areas (building dimensions and street widths) are taken from Voogt and Oke (1997) and building dimensions for the base case simulations are set up so as to preserve the complete to plan area ratio ( $A_c/A_p$ ) and plan area ratio ( $A_r/A_p$ ; roof area to plan area) for those sites. For the surface geometry sensitivity studies, the dimensions are varied according to the height to width ratio ( $H/W$ ) of the streets and the plan area ratio.

## 2.2 Modeled Urban Surface Temperatures

**2.2.1 Facet-averaged surface temperatures.** The surface temperatures are modeled using the urban canopy-layer climate model (UCLM) of Mills (1997). This model calculates the facet surface temperatures within a 3 x 3 array of buildings which themselves are surrounded by a solid wall for view factor and shading calculations (Mills 1997). The ground surface in this model is assumed to have homogeneous properties. All surfaces are assumed to be dry and no latent heat flux is modelled. Choices for model radiative and thermal parameters (Table 1) are based on those used by Masson *et al.* (2002) with depth averaging performed to provide representative values for the homogeneous material as assumed by the Mills model. The resultant modeled surface temperatures apply to the facet as a whole and are not subdivided into sunlit and shaded portions. The boundary conditions for the model are specified from measured data collected at the LI site.

Parameter	roof	Wall	ground
Surface	tar+gravel	brick	Asphalt + concrete
albedo	0.12	0.5	0.25
emissivity	0.92	0.90	0.94
conductivity ( $W m^{-1} K^{-1}$ )	0.06	0.80	1.21
heat capacity ( $J m^{-3} K^{-1} \times 10^6$ )	1.0	0.83	1.95
thickness (m)	0.1	0.2	0.3

Table 1. Input surface parameters: Light Industrial study area.

Tests with the UCLM compared to observations made at the LI study area showed reasonable agreement between model and observations when the internal building temperature was fixed at the average daily temperature, however some shaded walls (north and west-facing) were warmer than observations and the walls, especially the south and west walls, cooled too quickly in the late afternoon. Using a calculated internal building temperature as formulated in UCLM results in a substantial overestimation of wall temperatures in particular, as heat accumulates through the day in the building. However, the temperature *differences* between facets are represented remarkably well (Figure 1), including the late afternoon cooling that was overestimated with the fixed building temperature. Because anisotropy is critically dependent on the temperature differences between facets of the urban surface, we

use UCLM with a calculated internal building temperature for the analyses presented here.

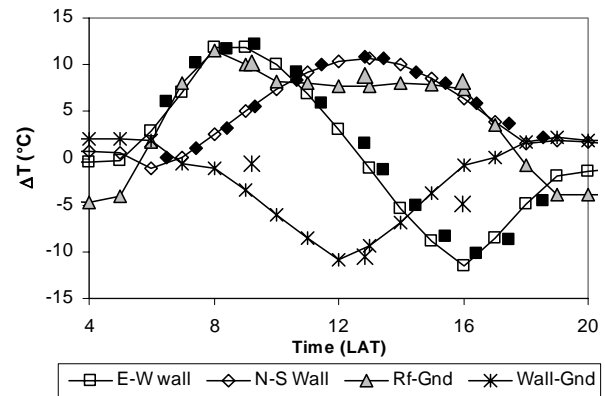


Figure 1. Modeled and observed facet temperature differences for facet pairs important to creating anisotropy, LI area. Solid symbols are observed values from ground-traverses. Large individually plotted points are observed values from airborne thermal imagery.

### 2.2.2 Within Facet Variations of Surface Temperature:

To assess the variability of surface temperatures at the sub-facet scale, we use a newly developed 3-D urban energy balance model TUF-3D (Krayenhoff 2005). This model has the ability to predict component surface temperatures for a variety of surface geometries and properties, weather conditions, and solar angles. It is composed of radiation, conduction and convection sub-models, and it matches the plane-parallel raster-type geometry of the SUM sensor-view model. The radiation sub-model utilizes the radiosity approach and accounts for multiple reflections and solar shading. Conduction is solved with a finite difference representation of the Fourier law of heat conduction, and convection is modelled by empirically relating the heat transfer coefficient to the momentum forcing and the building morphology. The 3-D cell structure of this model provides the capability of outputting surface temperatures for both sunlit and shaded areas of canyon surfaces as well as assessing the variability of surface temperature within individual facets, for example, across walls or between intersections and mid-block positions.

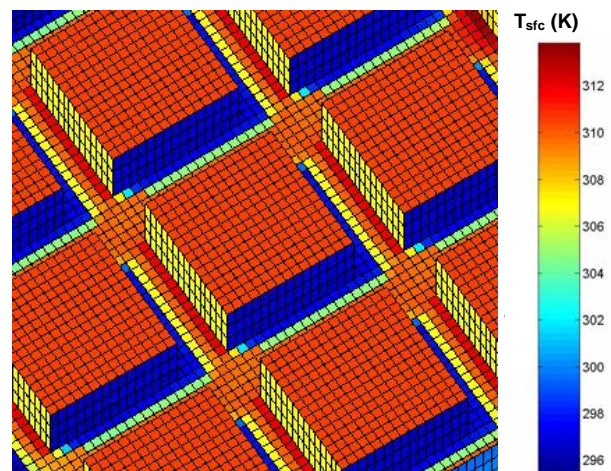


Figure 2. Sample surface temperature output from TUF-3D for the LI study area. View is from the NE at 0900 LAT.

### 2.3 Modeled Radiative Source Areas

Radiative source areas are modeled using the SUM surface-sensor-sun relations model (Soux *et al.* 2004). The SUM model calculates the view-factors for sunlit and shaded portions of the urban surface and can use externally-input GIS surface data, or an internal simplified representation of the urban surface. Radiative surface temperatures of the sunlit and shaded components of the urban surfaces must be provided to SUM from an independent source. Using this information SUM can generate estimates of the directional radiative temperature for a given sensor viewing position. When detailed surface geometries are provided, and observed facet temperatures are used, SUM shows good agreement with observations of thermal anisotropy (Figure 3).

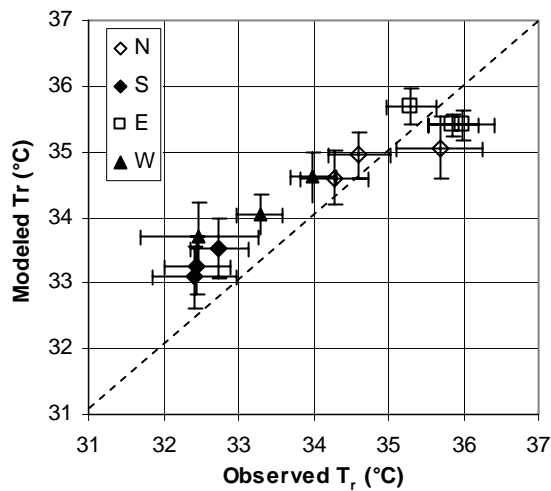


Figure 3. Modeled and observed radiative surface temperatures, LI study area, Aug. 15, 1992, 1600 LAT.

In this work, SUM is used with the simple internal urban surface structure to provide a match with that used in the urban canopy-layer model. A 1 m x 1 m x 1m grid resolution is used. Some adjustments are made to the absolute building dimensions within SUM in order to maintain the integer dimensions required by the model array and to preserve the H/W ratio of the streets specified in the energy balance model. The actual surface dimensions as used in SUM are shown in Table 2.

The SUM viewing parameters for the two sites are shown in Table 3. The sensor IFOV matches that used in an observational study (Voogt and Oke 1998). Here, the sensor height is increased to reduce the sensitivity of the output to the absolute position of the projected FOV onto the modelled building array.

SUM simulations are made for the nadir viewing position and then for 15° intervals in azimuth and 10° intervals in off-nadir angle from 5 – 45°. Anisotropy is represented as the maximum temperature difference or range from among all the viewing angles and azimuths tested. The standard deviation among all the modelled temperatures is also calculated; generally it shows similar variations to the range (see, e.g. Figure 6). The maximum anisotropy is usually observed for large off-nadir view angles in opposing directions, typically in the up- or down-sun azimuth view directions. SUM simulations are performed only in the morning with the expectation that results

would be similar, if not slightly smaller following solar noon because the temperature differences between facets tends to be symmetrical about solar noon, with perhaps some reduction in the temperature differences between facet pairs during the late afternoon, as roads warm relative to roofs, and north-facing walls warm through the day (Figure 1).

Downtown					
H/W	H	BL & BW	SW	$A_c/A_p$	$A_r/A_p$
1	15	18	15	1.99	0.30
1.67	15	18	9	2.48	0.44
2	14	18	7	2.61	0.52
3	15	18	5	3.04	0.61
4	16	18	4	3.38	0.67
5	15	18	3	3.45	0.74
Light Industrial					
0.25	7	30	28	1.25	0.27
0.5	7	30	14	1.43	0.46
0.6	6	25	10	1.49	0.51
0.75	9	30	12	1.61	0.51
1.0	7	30	7	1.61	0.66
1.25	10	30	8	1.83	0.62
1.5	9	30	6	1.83	0.69
2	8	30	4	1.83	0.78
3	9	30	3	1.99	0.83

Table 2. Surface dimensions (m) used in SUM and select non-dimensional surface parameters for the study areas in Vancouver. H = building height, BL = building length and width, and SW = street width must be integer values in SUM. Bolded values are those used in the energy balance model, with the remaining values set by H/W.

Parameter	Light Industrial	Downtown
FOV	12°	
Sensor Height	750 m	450 m
View angles	5 – 45, 10° steps	
View azimuths	15 – 345, 15° steps	
Array dimensions	400 x 400 m	300 x 300 m

Table 3. Input sensor characteristics for SUM.

## 3. RESULTS

### 3.1 Variation with Surface Geometry

Anisotropy as a function of canyon H/W geometry is shown in Figure 4 (LI study area) and Figure 5 (DT study area). Anisotropy generally increases as Z decreases, although this increase is not monotonic in all cases. In the LI area, of the geometries tested, a H/W = 1.0 results in the largest anisotropy. H/W ratios of 1.25 and 0.75 are characterized by substantially smaller anisotropies at small zenith angles. For the LI area the anisotropy is small for H/W > 2 and H/W < 0.5.

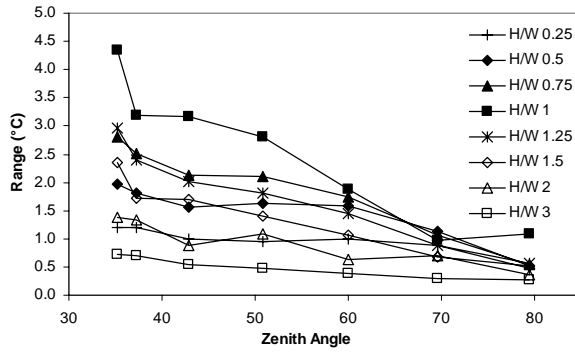


Figure 4. Variation of remotely observed surface temperature with variations in canyon H/W ratio. Surface geometry based on the LI study area with internal building temperature calculated.

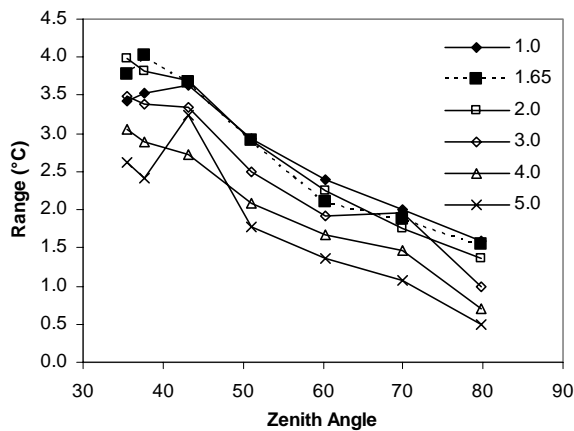


Figure 5. Thermal anisotropy for H/W variations of the DT study area. Base-case H/W shown by large solid square.

In the DT area, absolute values of anisotropy tend to be larger for the same H/W compared to the LI area. This appears to be related to the relative azimuth angle with the street orientation (which is roughly 45° from N-S, E-W); temperature differences between facet pairs are smaller than in the LI area, and plan area ratios are similar. For both study areas, the actual surface geometry (H/W = 1.65 DT and H/W = 0.6 LI) provides nearly the maximum anisotropy for the range of surfaces tested. As well, relatively low H/W ratios result in significant anisotropy in both study areas (and in some cases more anisotropy than larger H/W ratios), suggesting that substantial areas of real-world cities may be prone to having significant thermal anisotropy, not just the most densely built downtown areas.

Figure 6 plots results of the coupled model anisotropy for solar noon on the study day using surface geometry, thermal and meteorological inputs for the LI area and a range of plan area ratios (roof to total plan area of the building lot  $A_r/A_p$ ). The test keeps the building dimensions constant, varying only the lot area. The plan area ratios tested correspond to H/W of 0.33- 10. These results show two peaks in the anisotropy, near  $A_r/A_p = 0.25$  and 0.7 (corresponding to canyon H/W = 1 and 5) and a relative minimum between  $A_r/A_p = 0.4 - 0.45$  (corresponding to H/W = 1.66-2.0). The peak at the higher plan area ratio is larger, but is less typical of observed urban densities. For  $A_r/A_p < 0.5$ , more typical of urban areas, the variability of the modeled anisotropy is on the order of 30%.

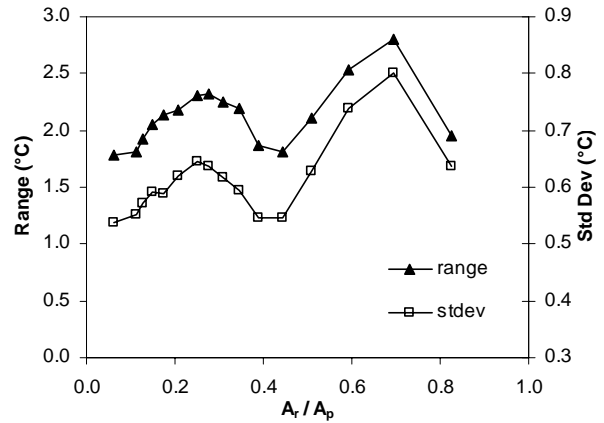


Figure 6. Thermal anisotropy for various plan area ( $A_r/A_p$ ) ratios (Solar zenith angle = 35°, Azimuth = 180°, Aug. 15, 1992).

### 3.2 TUF-3D Simulations.

Modeled surface temperatures from the UCLM are limited to facet averages, and therefore over- and underestimate temperatures of shaded and sunlit portions of the facets respectively that are “seen” by SUM. When facet average temperatures are input to SUM it has the impact of reducing the overall anisotropy. The TUF-3D model does not have this limitation and is designed so that eventually it will be able to provide a matching 3-D grid of surface temperatures (Figure 2) for use with SUM. In the test shown in Figure 7, temperatures are averaged for sunlit and shaded components of each facet, to more directly correspond to the standard input currently used by SUM. This test corresponds to the mid-day observation time from Voogt and Oke (1998) for the LI study area and so observational results may be plotted for comparison.

Results show (Figure 7) that for this particular case, the TUF-3D simulation provides nearly identical anisotropy estimates as the UCLM. However, the TUF model was run using a relatively small number of cells to represent the building walls, so in combination with the surface geometry of the study site, the capability of the model to provide within facet variations in temperature is somewhat underutilized in this case. The UCLMa simulation uses the same surface radiative and thermal properties as the previous simulations presented here, with the surface geometry set to match that used in TUF-3D and the SUM model (based on the surface parameters given in Masson et al. 2002). The UCLMb simulation adds matching surface radiative and thermal parameters, derived from depth averaging the values presented in Masson et al. 2002 in an attempt to define a single layer average that can correspond to the multi-layer TUF-3D model (but for which no check of the facet temperature differences with observations has been made). UCLMc is identical to UCLMa but with the shaded portions of roads and east and south walls replaced with canyon air temperature, instead of a facet averaged value. This simulation enhances model anisotropy over UCLMa and is similar to the results of UCLMb.

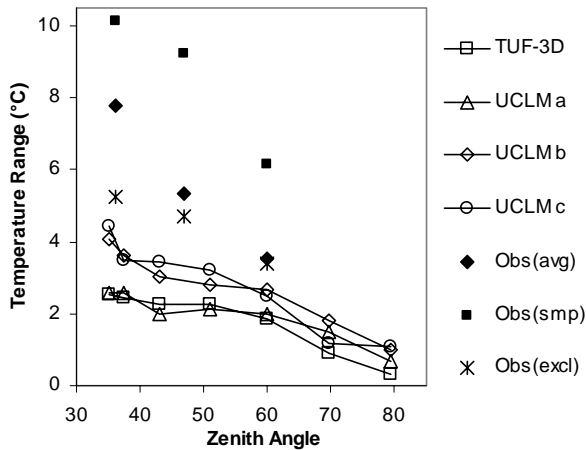


Figure 7. Anisotropy (temperature range) for the LI study area as generated by SUM + TUF-3D and SUM + UCLM modeled surface temperature. See text for explanation of the legend.

Compared to airborne observations from a series of 45° off-nadir viewing flight lines, the coupled model simulations substantially under-predict the thermal anisotropy. Observed anisotropy is largest when the range of temperatures is determined from all the individual images taken from the flight lines (Obs(smp) in the legend). When the anisotropy is determined from the mean temperature of each flight line, the anisotropy is reduced (solid diamonds). If the maximum and minimum values of the averaged flight line data are removed (Obs(excl)), in an attempt to exclude outliers, without biasing the overall data, a further reduction in anisotropy is noted, particularly for the lowest zenith angle. The large sensitivity of observed anisotropy highlights the importance of the microscale surface structure to the anisotropy: variable height buildings, some trees, pitched roofs and shading from sub-building scale structures all are likely to increase the observed anisotropy. The observations also include variation in surface radiative and thermal properties that also result in temperature variations that are contained within the observations but not yet incorporated in the model simulations.

#### 4. CONCLUSIONS

Two energy balance models are used to estimate surface temperatures for use with the SUM sensor view model in order to estimate urban thermal anisotropy for a range of urban surface geometries. Modelled temperature differences using the UCLM were shown to agree well with observed differences in the study areas, but there were differences between the absolute magnitudes of the modelled and observed temperatures.

The modelled anisotropy (using canyon H/W ratios) suggests that the study site geometries provided large anisotropy relative to other H/W ratios. Results of a test comparing the anisotropy for a range of plan area ratios (roof to building lot area) showed two peaks. Variation of the thermal anisotropy for plan area ratios most likely to characterize real cities was approximately 30%. The indication that anisotropy was relatively large for commonly observed urban geometries underscores the importance of anisotropy for large areal extents of urban surfaces, and not just those characterized by very tall surfaces and large H/W.

The modelled anisotropy for the light industrial study area substantially under-predicts compared to airborne observations. Factors that appear to be responsible for this discrepancy include: the simple urban surface representation, including lack of sub-building scale features, equal height buildings, no variation in surface properties between buildings or within facets. The capabilities of the newly available TUF-3D should provide the means to begin addressing these discrepancies in more detail.

#### REFERENCES

- Krayenhoff, E.S. 2005. Development of a micro-scale 3-D urban energy balance model and its application to the study of effective thermal anisotropy in urban environments. Unpublished M.Sc. Thesis, University of Western Ontario, London ON Canada.
- Lagouarde, J.P. et al. 2004. Airborne experimental measurements of the angular variations in surface temperature over urban areas : case study of Marseille (France). *Rem. Sens. Environ.* 93, pp. 443-462.
- Masson, V., Grimmond, C.S.B, and T.R. Oke, 2002. Evaluation of the Town Energy Balance (TEB) scheme with direct measurements from dry districts in two cities. *J. Appl. Meteorol.*, 41, pp. 1011-1026.
- Mills, G. 1997: An urban canopy-layer climate model. *Theor. Appl. Climatol.*, 57, pp. 229-244.
- Soux, A., Voogt, J.A. and T.R. Oke, 2004: A model to calculate what a remote sensor 'sees' of an urban surface. *Bound. Layer-Meteorol.*, 111, pp. 109-132.
- Voogt, J.A. and T.R. Oke, 1998: Effects of urban surface geometry on remotely-sensed surface temperature. *Int. J. Rem. Sens.*, 19, pp.895-920.
- Voogt, J.A. and T.R. Oke, 1997: Complete urban surface temperatures. *J. Appl. Meteorol.*, 36(10), pp. 1117-1132.